Chemical Physics Letters 517 (2011) 180–185

Contents lists available at SciVerse ScienceDirect

Chemical Physics Letters

journal homepage: www.elsevier.com/locate/cplett

Heterogeneity and viscosity decoupling in (acetamide + electrolyte) molten mixtures: A model simulation study

Tamisra Pal, Ranjit Biswas *

Department of Chemical, Biological and Macromolecular Sciences, S. N. Bose National Centre for Basic Sciences, Block-JD, Sector-III, Salt Lake, Kolkata 700098, India

ARTICLE INFO

Article history:
Received 1 October 2011
In final form 1 November 2011
Available online 4 November 2011

ABSTRACT

Recent time-resolved fluorescence experiments with (acetamide + electrolyte) melts have revealed pronounced decoupling of solute and solvent dynamics from medium viscosity. Here we examine the diffusion–viscosity (D–η) relationship by performing molecular dynamics simulations approximating acetamide molecules as dipolar Lennard–Jones (L–J) spheres and ions as L–J spheres with point charges. Interestingly, eventhough simulated viscosities are found to be approximately an order of magnitude lower than those from experiments, simulated diffusion coefficients are larger by ~500–4000 times than the hydrodynamic predictions using the experimental viscosities. Simulated particle motions exhibit strong dynamic heterogeneity via pronounced non-Gaussian character of particle displacements. A signature of an extremely fast dipole orientation is also observed.

1. Introduction

Binary and ternary mixtures of acetamide with electrolytes are well-known examples of supercooled melts around room temperature [1–7]. These melts are characterized by pronounced microscopic solution heterogeneities [2–4,8] and glass transition temperatures (T_g) in the range, $\sim 190 < T_g\ (K) < 250$ [6,7,9,10]. Depending on mixture composition and temperature, viscosity (η) of these melts varies between ~4 and 250 cP, and exhibits, as typical for fragile glass formers, a non-Arrhenius temperature dependence [6,7]. Recent time-resolved fluorescence measurements have revealed a strong decoupling of both solute and solvent dynamics from medium viscosity [11–13]. This is quite reminiscent of frequent observations in deeply supercooled neat liquids [14–16] and, therefore, the observed non-hydrodynamic behavior might be linked to the spatial and temporal heterogeneities of these melts. Interestingly, eventhough presence of strong spatial heterogeneities in these melts have been suggested by several earlier experimental studies [1–4,8], no measurements or simulations, similar to those for ionic liquids [17–22], have been carried out so far to better understand the heterogeneity and their effects on chemical events in these multi-component mixtures. Needless to say, a quantitative understanding of heterogeneities and their implications on transport properties is necessary for developing these melts into useful dielectric materials and subsequent applications in technology.

In this Letter, we report results from our molecular dynamics simulations on viscosity decoupling of diffusion in binary and ternary molten mixtures of acetamide (CH_3CONH_2) with sodium thiocyanate (NaSCN) and potassium thiocyanates (KSCN) at 318 K. Three different mixtures of the following general formula, $0.75CH_3CONH_2 + 0.25[fKSCN + (1-f)NaSCN]$ with f (fraction of K^+) = 0, 0.2 and 0.6, have been considered. Note that these are the melt compositions and temperature at which the fluorescence experiments reported in [11] have been carried out. Composition dependence of the spatial distributions of the ions and solvent particles, their diffusion coefficients, and mixture viscosities have been simulated in order to understand the ion–solvent interactions present in these systems. Dynamic heterogeneity is reflected in the large values of non-Gaussian parameter ($\alpha(t)$) and pronounced deviations from the Gaussian distribution (with respect to particle displacement) of the self part of the van Hove correlation function ($G_s(\mathbf{r},t)$) in the simulated particle motions [23,24]. Eventhough strong non-Gaussian characteristics have been found in the particle motions, no rattling within a cage, as typically seen in supercooled systems [25,26] and ionic liquids [27,28], could be detected in the present model simulations. Moreover, similar to earlier findings for mixed alkali silicate glasses [29–31], addition of foreign ion (here K^+) suppresses the long-range motions of other ions (Na^+ and SCN^-) and solvent particles, the extent of suppression being the largest at the lowest K^+ concentration considered.

Note here that the pair potential between two acetamide molecules is approximated by that between two dipolar L–J spheres, whereas pair interaction between ions is assumed to be given that between two singly-charged L–J spheres. Such modeling of pair potentials completely neglects shape anisotropy, molecular

* Corresponding author.
E-mail addresses: rbsnbc@gmail.com, ranjit@bose.res.in (R. Biswas).

0009-2614/$ - see front matter © 2011 Elsevier B.V. All rights reserved.
doi:10.1016/j.cplett.2011.11.002

flexibility and other atomic details and therefore excludes the possibility of reproducing the static heterogeneity revealed by various experiments with these melts [2–4,8]. This will have implications on various properties of this melt, most directly on the viscosity, because structural heterogeneity is known to substantially affect this transport quantity [32,33]. However, longer-ranged ion–ion ($u_{ii} \propto r^{-1}$), ion–dipole ($u_{id} \propto r^{-2}$) and dipole–dipole ($u_{dd} \propto r^{-3}$) interactions are expected to dominate the energetic and dynamic aspects of these melts and thus a qualitative understanding of the D–η relationship may be achieved even without considering the detailed chemical interactions. Moreover, the model considered here for (acetamide + electrolyte) melts is similar in spirit to a recent coarse-grained representation of an idealized ionic liquid [27] which produced not only reasonable agreement between simulations and experiments on liquid structural and energetic properties but also on solute-based dynamics. In addition, consideration of only L–J interaction between particles in a simulation study [34] has been found to generate a qualitative understanding of the physical picture behind the cooperative blockage and jump dynamics [29,30] associated with the conductivity in mixed alkali glasses. Therefore, use of simple model potentials for studying dynamics in complex systems is not new. Our primary motivation here is to generate a qualitative understanding of the experimentally observed fractional viscosity dependence (of the medium dynamics) in these melts while being computationally economical.

2. Simulation details

A mixture of 384 acetamide molecules and 64 ion pairs (a total of 512 particles) were simulated by using a home-developed code in the canonical (NVT) ensemble at 318 K (Nose–Hoover thermostat) with box-length adjusted to produce the experimental density [6] of these melt mixtures at a given composition. Such compositions correspond to solutions with electrolyte present at $\sim 10^{-3}$ mol/l concentration. Here N denotes the total number of particle in the system, V the volume and T the absolute temperature. Periodic boundary conditions were employed and equations of motion integrated following the Verlet leapfrog integration scheme using a time step of $\sim$2 fs. Equilibration was done for 1 ns and the production run for 3 ns. Longer-ranged interactions were treated via the standard Ewald method [35,36]. The interaction potentials between a pair of ions, a pair of dipolar solvent molecules, and between a solvent dipole and an ion were respectively approximated as

$$u_{\text{ion-ion}}(r_i, r_j) = 4\varepsilon_{ij}\left[\left(\frac{\sigma_{ij}}{r_{ij}}\right)^{12} - \left(\frac{\sigma_{ij}}{r_{ij}}\right)^{6}\right] + \frac{q_i q_j}{r_{ij}}, \quad (1)$$

$$u_{\text{dipole-dipole}}(\mu_i, \mu_j) = 4\varepsilon_{ij}\left[\left(\frac{\sigma_{ij}}{r_{ij}}\right)^{12} - \left(\frac{\sigma_{ij}}{r_{ij}}\right)^{6}\right] + \frac{\mu_i \mu_j}{r_{ij}^3}, \quad (2)$$

$$\text{and } u_{\text{ion-dipole}}(q_i, \mu_j) = 4\varepsilon_{ij}\left[\left(\frac{\sigma_{ij}}{r_{ij}}\right)^{12} - \left(\frac{\sigma_{ij}}{r_{ij}}\right)^{6}\right] + \frac{q_i \mu_j}{r_{ij}^2}. \quad (3)$$

In the above expressions q and μ represent charge and dipole moment, respectively, i and j different particles (ion or/and solvent dipole) and r_{ij} distance between two such particles. The L–J lengthscales (σ_{ij}) and energy parameters (ε_{ij}) were obtained by using the Lorentz–Berthelot [35] combination rule (that is, $\sigma_{ij} = \frac{\sigma_i + \sigma_j}{2}$ and $\varepsilon_{ij} = \sqrt{\varepsilon_i \varepsilon_j}$) from the known individual L–J parameters [11,37–39]. μ = 3.7 D [11].

3. Results and discussion

We present in Figure 1 the simulated Na^+–Na^+ and CH_3CONH_2–CH_3CONH_2 radial distribution functions ($g(r)$) at f = 0, 0.2 and 0.6

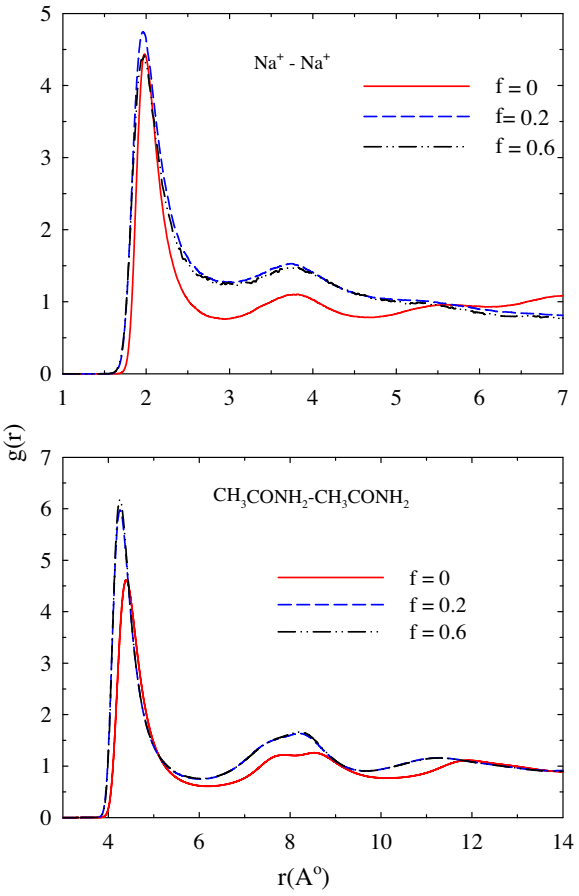

Figure 1. Composition dependence of the center-of-mass radial distribution function (RDF), $g(r)$ for Na^+ and solvent (acetamide) particles present in the (acetamide + sodium/potassium thiocyanate) melt at 318 K. Solid, dashed and dash-dot lines represent RDFs at f = 0, 0.2, 0.6, respectively (also indicated in each of the panels). The RDFs are color-coded (online only). See Figures S1 and S2 of the Supporting material for $g(r)$ of other species in the melt.

for the melt $0.75CH_3CONH_2 + 0.25[f\text{KSCN} + (1-f)\text{NaSCN}]$ at 318 K. K^+–K^+, SCN^-–SCN^-, Cation–anion and ion–solvent $g(r)$ are shown in Figures S1 and S2 (Supplementary data). Data in these figures clearly indicate that the addition of K^+ influences the spatial distribution of particles, the effect being the strongest at the lowest concentration of KSCN. Note that while the addition of K^+ enhances the first peak height and broadens the simulated $g(r)$ for Na^+–Na^+, SCN^-–SCN^-, Na^+–SCN^- and CH_3CONH_2–CH_3CONH_2, increase in K^+ concentration in melt reduces and narrows those for Na^+–CH_3CONH_2 and K^+–CH_3CONH_2. Moreover, K^+–K^+ and K^+–SCN^- radial distribution functions (RDFs) do not show any appreciable change upon increasing the KSCN concentration. The enhancement and broadening of ion-ion and solvent–solvent RDFs along with the insignificant changes in those for K^+–K^+ and K^+–SCN^- suggest enhanced interactions between these species upon addition of KSCN and thus much less ideal mixing. The reduction by a factor of $\sim$2 of the first peak height of Na^+–CH_3CONH_2 RDF upon addition of K^+ (see Figure S1) seems to suggest stronger interaction between acetamide and K^+ than that between Na^+ and acetamide. A decrease in diffusion coefficient of acetamide upon increase in f and a relatively smaller diffusion coefficient for K^+ than Na^+ (shown later) further support this view as mobility of these alkali metal ions in common polar solvents shows quite the opposite trend [40]. The second peak of the simulated CH_3CONH_2–CH_3CONH_2 $g(r)$ at f = 0 appears non-regular and suggests presence of slight disorder [41,42]. Interestingly, experimental studies with this melt at f = 0

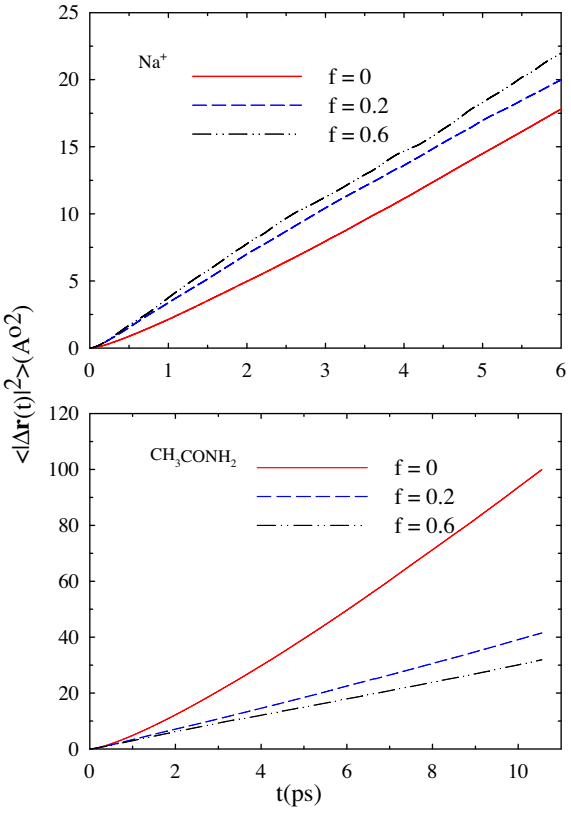

Figure 2. Composition dependent center-of-mass mean squared displacements (MSD) for Na^+ and acetamide for the melt under study. As in Figure 1, the color-code is only for online. MSDs for K^+ and SCN^- are provided in Figure S3 of the Supporting material.

have indicated presence of substantial disorder in solution structure [4]. Simulations incorporating detailed atomic interactions are therefore required for a better understanding of the static disorder (and thus spatial heterogeneity) of these systems.

Next we present in Figure 2 the composition dependent mean squared displacements (MSDs) for Na^+ and solvent particles. MSDs for the other species are provided in the supporting material (Figure S3). The MSDs have been calculated from the time-dependent center-of-mass positional vectors $(\vec{r}_i^c(t))$, $\left\langle |\Delta\vec{r}(t)|^2 \right\rangle = \frac{1}{N}\left\langle \sum_{i=1}^{N} |\vec{r}_i^c(t) - \vec{r}_i^c(0)|^2 \right\rangle$. Note that none of the MSDs shown here exhibit 'rattling in a cage' motion so typical for alkali glasses [25], supercooled systems [26] and ionic liquids [27,28]. It is again evident that the addition of K^+ influences the MSDs and thus the diffusion coefficient (because $D = [\frac{1}{6t}(\left\langle |\Delta\vec{r}(t)|^2 \right\rangle)]_{t\to\infty}$) of each of the species present in the melt, the most affected being those of the acetamide molecules. The corresponding velocity autocorrelation function (Figure S4, upper panel, supporting material) also shows a similar effect. Simulated diffusion coefficients (D) summarized in Table 1 reveals that SCN^- is the most efficient among the diffusing ions in this melt. Moreover, while D for acetamide reduces substantially, an over-all increase (small though) in D for the ions is observed for changing f from 0 to 0.6 in this melt. This is in qualitative agreement with experiments [43] which report enhancement of electrical conductivity upon replacement of Na^+ by K^+ in this melt (see Figure S4, lower panel). However, simulated diffusion coefficients for K^+, present in the current melt at millimolar concentration, is ~5 times larger than that estimated from the measured conductivity of centi-molar solutions of potassium chloride in molten acetamide at ~367 K [44]. Also, simulated D for Na^+ (also present at milli-molar concentration) is more than an order of magnitude larger than the measured value in *N*-methylacetamide (NMA) at ~313 K [45]. These results contradict the hydrodynamic predictions because η_{melt} at 318 K is larger than η_{NMA} at ~313 K [45] and $\eta_{Acetamide}$ at ~367 K [11] and, therefore, suggest participation of non-hydrodynamic mechanism for particle movement.

A comparison in Table 2 among the simulated diffusion coefficients (D_{simu}) and those from hydrodynamics (D_{cal}) calculated after using the simulated and measured viscosities (η_{simu} and η_{expt}, respectively) further reflects the inefficiency of the hydrodynamics in describing the particle diffusion in the present melt. The comparison is a representative one (shown only for $f = 0$) and the viscosity has been simulated from the stress tensor autocorrelation function as described in the literature [24]. At this composition ($f = 0$), we find $\eta_{simu} = 20$ cP, a value more than an order of magnitude less than in experiments ($\eta_{expt} = 235$ cP) [6]. This underestimation is expected because of the non-consideration of the atomistic details in the interaction potentials but the simulated value will be sufficient to show the break-down of the hydrodynamic description for particle diffusion in this melt. Note that the simulated diffusion coefficients for CH_3CONH_2, Na^+ and SCN^- are larger by factors of ~4300, ~500, ~3100, respectively, than the corresponding hydrodynamic (Stokes–Einstein) [24] predictions using η_{expt}. These differences are reduced by the factor, $\eta_{expt}/\eta_{simu} \approx 12$, when the simulated viscosity replaces the experimental one in the Stokes–Einstein relation. The simulated diffusion coefficients are still much larger than the hydrodynamic predictions and strongly indicate partial decoupling from the medium viscosity.

Next we explore the dynamic heterogeneity as a probable reason for the observed break-down of the Stokes–Einstein relation via examining the time-evolution of the self-part of the van Hove correlation function, defined as [24]

$$G_s(\vec{r},t) = \frac{1}{N}\left\langle \sum_{i=1}^{N} \delta(\vec{r}_i^c(t) - \vec{r}_i^c(0) - \vec{r}) \right\rangle, \quad (4)$$

which describes the probability of locating the center-of-mass of a particle at r^c at time t given that it was at the origin $r^c(0)$ at $t = 0$. Because of the Maxwell–Boltzmann velocity distribution in the free particle limit (that is, $\Delta r \to 0$ and $t \to 0$) and hydrodynamic behavior at $t \to \infty$, $G_s(\vec{r},t)$ exhibits Gaussian distribution with particle displacement, $\Delta\vec{r}(t)$. Additionally, $G_s(\vec{r},t)$ for most liquids at normal condition retains the Gaussianity at all times [28]. Traditionally, strong deviations from Gaussian behavior in supercooled liquids at

Table 1
Composition dependent simulated diffusion coefficients for ions and acetamide particles in $0.75CH_3CONH_2 + 0.25[fKSCN + (1-f)NaSCN]$ at 318 K. Diffusion coefficients have been calculated from both the MSD and VACF routes. The error bars (standard deviation about the mean) have been estimated from block averaging.

	D ($f = 0.0$) $\times 10^4$ (cm^2/s)			D ($f = 0.2$) $\times 10^4$ (cm^2/s)			D ($f = 0.6$) $\times 10^4$ (cm^2/s)		
	MSD	VACF	Average	MSD	VACF	Average	MSD	VACF	Average
CH_3CONH_2	1.79 ± 0.19	1.94 ± 0.40	1.87 ± 0.29	0.68 ± 0.19	0.73 ± 0.37	0.71 ± 0.28	0.50 ± 0.22	0.51 ± 0.27	0.51 ± 0.25
Na^+	0.54 ± 0.15	0.51 ± 0.13	0.53 ± 0.14	0.53 ± 0.19	0.53 ± 0.15	0.53 ± 0.17	0.59 ± 0.13	0.54 ± 0.16	0.57 ± 0.15
K^+				0.51 ± 0.10	0.50 ± 0.15	0.51 ± 0.13	0.56 ± 0.19	0.52 ± 0.15	0.54 ± 0.17
SCN^-	1.46 ± 0.28	1.44 ± 0.40	1.45 ± 0.34	1.53 ± 0.22	1.55 ± 0.19	1.54 ± 0.21	1.59 ± 0.26	1.71 ± 0.22	1.65 ± 0.24

Table 2
Break-down of Stokes–Einstein relation for particle diffusion in (acetamide + sodium/potassium thiocyanates) molten mixtures at $f = 0$ and 318 K. Error bars have been calculated by following the method as mentioned for Table 1.

Species	$D_{cal} = \frac{k_B T}{6\pi\eta r}$ $(cm^2/s) \times 10^7$ From $\eta_{simu} = 20$ cP	$D_{cal} = \frac{k_B T}{6\pi\eta r}$ $(cm^2/s) \times 10^7$ From $\eta_{expt} = 235$ cP	D_{simu} $(cm^2/s) \times 10^7$
CH_3CONH_2	5.1533	0.438	1870.65 ± 290
Na^+	12.0066	1.022	525.83 ± 140
SCN^-	5.4169	0.461	1453.40 ± 340

intermediate times have been attributed to dynamic heterogeneity [46] and qunatified by the following non-Gaussian parameter [23]

$$\alpha(t) = \frac{3}{5}\frac{\left\langle |\Delta\vec{r}(t)|^4 \right\rangle}{\left\langle |\Delta\vec{r}(t)|^2 \right\rangle^2} - 1. \quad (5)$$

For a Gaussian $G_s(\vec{r}, t)$ as in the cases of random walk or homogeneous harmonic vibrations [26], $\alpha(t) = 0$. For hot liquids, $\alpha(t) = 0$ for both at $t = 0$ and $t = \infty$ but $\alpha(t) = 0.2$ (a maximum) at intermediate times [26].

Figure 3 depicts the composition dependence of $\alpha(t)$ simulated for Na^+ and K^+ ions present in the current melt. Simulated $\alpha(t)$ s for SCN^- and acetamide are shown in the Supporting material (Figure S5). Eventhough the data are noisy because of insufficient averaging, the multi-peak (or peak *plus* a shoulder) structure of $\alpha(t)$ is evident. Large values of $\alpha(t)$ at intermediate times ($\sim 10 \leqslant t/ps \leqslant 1000$) indicate presence of varying rates of motion for the particles (dynamic heterogeneity) at each of the compositions considered. Note $\alpha(t)$ for SCN^- at $f = 0.6$ has not decayed to zero even after ~2 ns, indicating extremely sluggish dynamics for this ion and warrants a much longer simulation run. The multi-peak (or peak + shoulder) structure has already been observed in simulations of mixed alkali silicate glasses and explained in terms of localization of jumps of shorter and longer lengthscales at short and long times, respectively [29]. Also note that the scales of $\alpha(t)$ for different species are strikingly similar to those reported in [29] but quite different from the simulated results for an ionic liquid, 1-ethyl-3-methylimidazolium nitrate [47]. Additionally, the effects on $\alpha(t)$ is the most dramatic at $f = 0.2$, and dilution of one of the alkali metal ions by the other moves the peak of $\alpha(t)$ towards shorter times. However, increase of f shifts the peak for SCN^- towards longer times and leads to an emergence of a shoulder for CH_3CONH_2 around 10 ps. The $\alpha(t)$ profiles shown here therefore indicate that dynamic heterogeneity in this melt is present over a wide range of timescale, and motions of different lengthscales for each of the particles (ions and solvent) contribute to the observed partial decoupling of D from η.

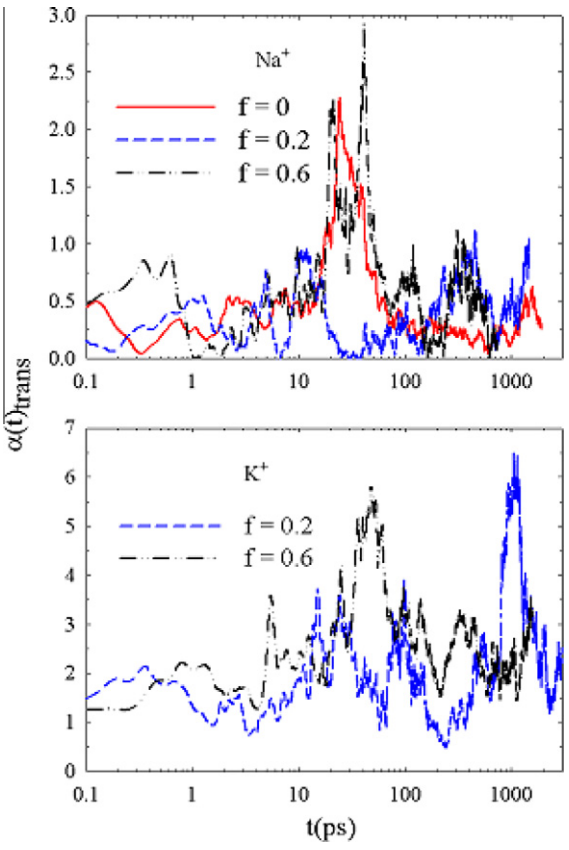

Figure 3. Composition dependence of the non-Gaussian parameter, $\alpha(t)$, for alkali metal ions present in the melt, $0.75CH_3CONH_2 + 0.25[fKSCN + (1-f)NaSCN]$ at 318 K. $\alpha(t)$ has been calculated by using Eq. (5) described in the text. Colors are for online. Simulated data are noisy because of insufficient averaging. See Figure S5, Supporting material, for $\alpha(t)$ s associated with SCN^- and acetamide. Note that better averaging via longer runs will remove the noise but not alter the qualitative understanding generated by the present curves.

The deviation from the Gaussian distribution with particle displacement is further elaborated in Figure 4 where the simulated composition dependent self-part of the van Hove function, $G_s(\vec{r}, t)$, for each of the ions and acetamide are shown, for a time where the respective $\alpha(t)$ s exhibit maxima in the intermediate time scale, and compared with the corresponding Gaussian approximation [28], $G_s^0(r,t) = [3/2\pi\langle|\Delta\vec{r}(t)|^2\rangle]^{3/2}\exp(-3r^2/(2\langle|\Delta\vec{r}(t)|^2\rangle))$. Note that at these times the deviation from Gaussian distribution is expected to be the most pronounced. It is clear that simulated distributions deviate strongly from the Gaussian approximation and show significant composition dependence. Of particular interest is the suppression of the large lengthscale motions for K^+ with f which is qualitatively similar to that found for mixed alkali silicate glasses [29] and can be attributed to the 'cooperative blockage' of the large jumps. In fact, relatively large lengthscale motions are increasingly becoming non-accessible with varying degree for all the ions and acetamide with f in this melt. A comparison between the simulated and calculated curves also reveal that the most pronounced effects are felt by those ions which are present at the dilute limit. Previous studies [30,34] have shown that presence of foreign ions at higher concentration leads to the suppression of both jump length and collective dynamics. This might be the reason behind the drastic deviation of $G_s(\vec{r}, t)$ for Na^+ from Gaussian distribution at $f = 0.6$ around 40 ps but much tender one for K^+ at the same composition and similar time. The role of concentration is further supported by the relatively weaker deviation of simulated $G_s(\vec{r}, t)$ from the Gaussian ones for SCN^- and CH_3CONH_2 whose concentrations remained unaltered during the change of mixture composition. Figures 3 and 4 might therefore jointly suggest that the addition of K^+ pushes the medium dynamics towards faster timesacles via localizing the jumps between neighboring regions and thereby effectively shortening the timescales of dynamical events. This is probably the reason for the experimental observation of faster solute and solvent dynamics with f in this melt [11].

A visual sense of the heterogeneity in particle motion is presented in Figures S6 and S7 (Supporting material) where 1 ns

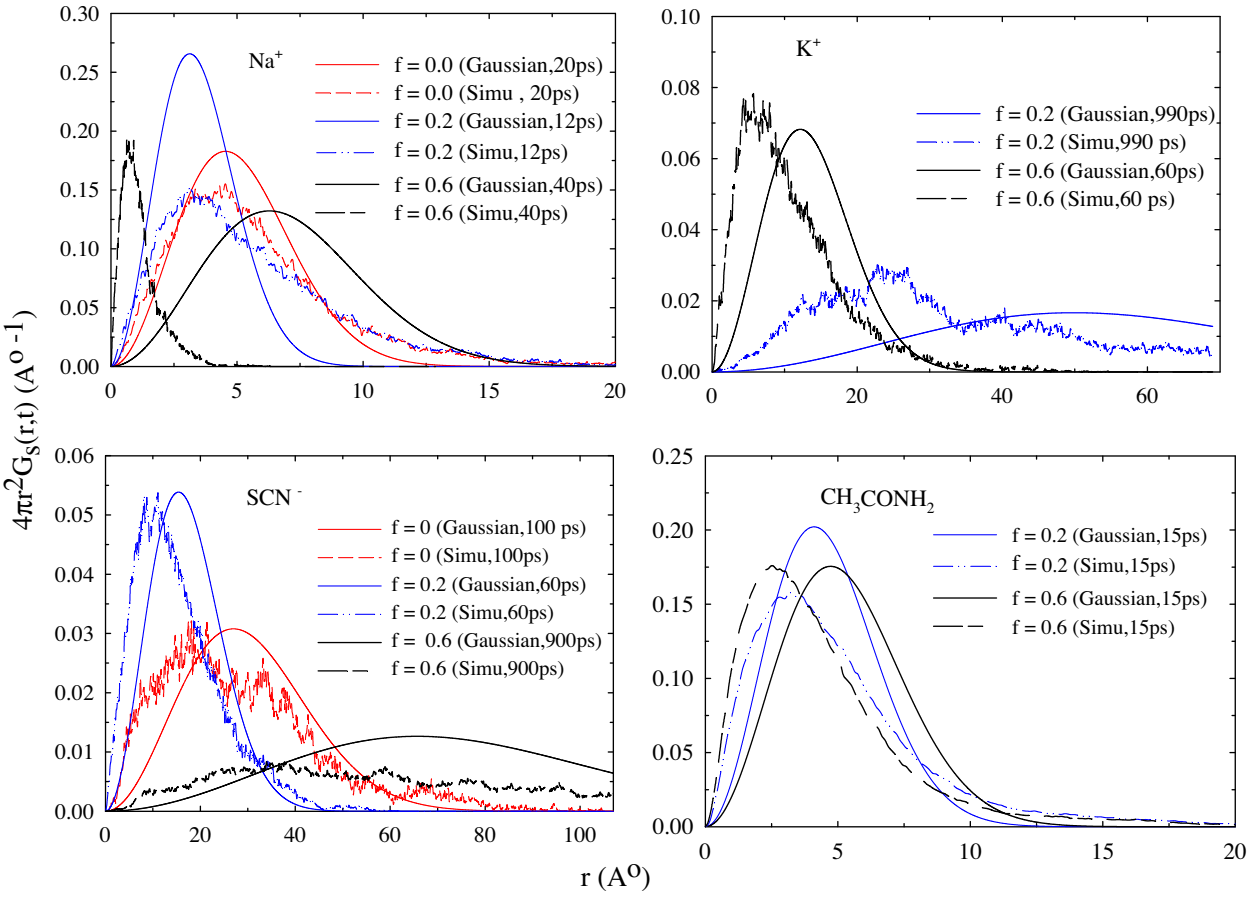

Figure 4. Effects of K^+ concentration on the self-part of the van Hove function, $G_s(\vec{r},t)$, for each of the species present in the molten mixtures of (acetamide + sodium/potassium thiocyanate) at 318 K. Smooth solid lines (color online) denote the calculated $G_s(\vec{r},t)$ assuming Gaussian distribution with respect to the particle displacement as described in the text. Simulated and calculated $G_s(\vec{r},t)$ are shown at times where the corresponding $\alpha(t)$ attains a maximum value. These times are indicated in the legends. Note the simulated data for ions appear noisy which become nearly smooth for acetamide because of better averaging due to relatively larger number of particles.

trajectories associated with the center-of-mass motions of a few arbitrarily selected ions (Na^+, K^+ and SCN^-) and CH_3CONH_2 particles are shown for this melt at $f = 0.2$ and 318 K. These representative trajectories clearly indicate jump motions for ions (particularly for Na^+ and K^+) and heterogeneity in translational motion of all the particles. Note that in accordance with the time profile of MSDs presented in Figure 2, these trajectories also do not suggest any presence of rattling in a cage motion. However, some particles are seen to be more mobile (judged by the length covered in 1 ns) than others. The slow and fast particles in these mixtures, as in supercooled systems [14] and ionic liquids [28], might also be spatially correlated. This requires further investigation.

We next explore the timescales associated with the solvent dipolar rotation via following the relaxation of the normalized collective dipole moment autocorrelation function defined as [24]

$$\Phi(t) = \frac{\left\langle \vec{M}(0)\cdot\vec{M}(t)\right\rangle}{\left\langle |\vec{M}(0)|^2\right\rangle}, \tag{6}$$

where the time dependent collective dipole moment ($\vec{M}(t)$) is the sum over all the molecular dipole moments, $\vec{M}(t) = \sum_i^N \vec{\mu}_i(t)$. Note that $\Phi(t)$ is connected to the experimentally measured frequency dependent dielectric function ($\varepsilon(\omega)$) via the relation, $\varepsilon(\omega) = 1 + \frac{4\pi}{3Vk_BT} L[-\frac{d}{dt}\Phi(t)]$, where L denotes Fourier–Laplace transform. In addition, $\varepsilon(\omega)$ and polar solvation energy relaxation measured via time-resolved fluorescence experiments are intimately connected [11]. Since the available dielectric relaxation data [1] cannot provide any information regarding the short time dynamics of this melt because they were obtained via using rather a narrow frequency coverage (10^{-1}–10^8 Hz), we have followed the time evolution of $\Phi(t)$ mainly to justify the ultrafast solvation timescale suggested by our recent experiments [11]. We cannot, however, explore the reported slow timescale (>10 ns) [1] as they are too slow to be accessed by the present simulations. Figure 5 demonstrates this aspect where the simulated $\Phi(t)$ at $f = 0$ are shown for different temperatures. Note the decays shown in this figure are fitted lines through the actual simulated data (presented in the Supporting material, Figure S8). The short time $\Phi(t)$ decays are shown separately in the bottom panel for better representation of the extremely fast relaxation at the early stage. It is evident from this figure that eventhough none of the $\Phi(t)$ decays are complete within the present time window, both ultrafast and ultraslow timescales exist in this melt, particularly at lower temperatures. Moreover, the longtime decay shows the expected temperature dependence. Bi-exponential fit to these incomplete decays have been found to produce one timescale roughly in the 2–10 ps range and the other in the 0.3–1 ns range. Although the incomplete decay suggests presence of an even longer timescale, the simulated short time dynamics qualitatively support the experimental suggestion [11] that early part of the solvation energy relaxation of a laser-excited polar dye in this melt occurs in picosecond or even faster timescale. According to the simulated decay of $\Phi(t)$, an extremely rapid component of the dipolar solvent rotation provides a channel for such a fast solvation energy relaxation in this melt.

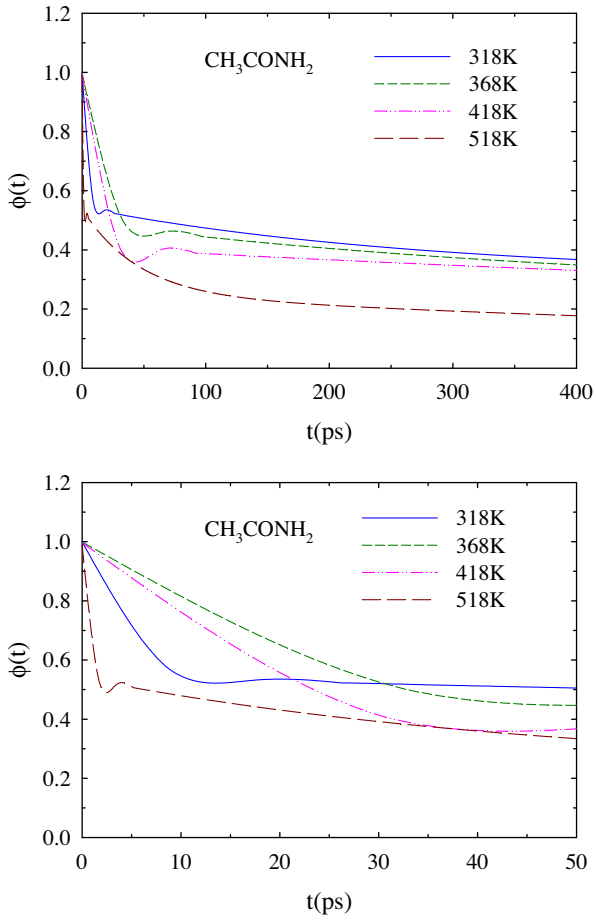

Figure 5. Temperature dependence of the relaxation of the collective dipole moment autocorrelation function, $\Phi(t)$, for acetamide in this melt at $f = 0$ and 318 K. Note the fitted data through the simulated curves (shown in Figure S8, Supporting material) are presented to avoid cluttering due to noise. While the upper panel shows the data for the full time window accessed by the present simulations, the lower panel specifically shows the early time dynamics. Data representations are indicated inside each of the panels and colors are for online only.

4. Conclusion

In summary, the present work shows that the dynamic heterogeneity is one of the responsible factors for the partial decoupling between the diffusion and viscosity coefficients in these melts. The decoupling of average solvation and rotation times for a polar solute in this melt at various compositions reflected in recent experiments [11,13] may be explained in terms of the dynamic heterogeneity observed in the present model simulation studies. The simulated decay of the collective dipole moment autocorrelation function indicates the presence of ultrafast polarization relaxation in this melt which was not explored before. It should, however, be kept in mind that eventhough various aspects of non-Gaussian parameter and the self-part of the van Hove correlation function for this melt are qualitatively similar to those found in mixed alkali silicate glasses, the simulated mean squared displacements for the ions or solvent particles never showed any indication of rattling within a cage. Simulations with more number of particles than considered here are not likely to alter the qualitative character of these results as evidences for secondary or no system size effects on ion motions in glassy systems already exist [25,30]. The role of the spatial heterogeneity remained unexplored because of the use of model interaction potentials in the present work. Limited simulation runs did not allow to access the slowest timescales associated with the dipolar relaxation in these systems. Moreover, relations between particle jump, local stress relaxation and wavenumber dependence of it [48–50] needs to be explored.

Acknowledgements

The authors are grateful to Prof. M. Maroncelli, Penn. State University and Dr. R.K. Murarka, IISER-Bhopal for insightful discussion, and Dr. P. Mahadevan, SNBNCBS for computational help.

Appendix A. Supplementary data

Supplementary data associated with this article can be found, in the online version, at doi:10.1016/j.cplett.2011.11.002.

References

[1] A. Amico, G. Berchiesi, C. Cametti, A.D. Biasio, J. Chem. Soc. Faraday Trans. 2 83 (1987) 619.
[2] G. Berchiesi, M.D. Angelis, G. Rafaiani, G. Vitali, J. Mol. Liq. 51 (1992) 11.
[3] G. Berchiesi, F. Farhat, M.D. Angelis, J. Mol. Liq. 54 (1992) 103.
[4] G. Berchiesi, J. Mol. Liq. 83 (1999) 271.
[5] F. Catellani, G. Berchiesi, F. Pucciarelli, V. Bartocci, J. Chem. Eng. Data 26 (1981) 150.
[6] G. Kalita, N. Rohman, S. Mahiuddin, J. Chem. Eng. Data 43 (1998) 148.
[7] G. Kalita, K.G. Sarma, S. Mahiuddin, J. Chem. Eng. Data 44 (1999) 222.
[8] G. Berchiesi, G. Rafaiani, G. Vitali, F. Farhat, J. Therm. Anal. 44 (1995) 1313.
[9] S. Mahiuddin, J. Chem. Eng. Data 41 (1996) 231.
[10] G.E. McManis, A.N. Fletcher, D.E. Bliss, M.H. Miles, J. Electroanal. Chem. 190 (1985) 171.
[11] B. Guchhait, H.A.R. Gazi, H.K. Kashyap, R. Biswas, J. Phys. Chem. B 114 (2010) 5066.
[12] H.A.R. Gazi, B. Guchhait, S. Daschakraborty, R. Biswas, Chem. Phys. Lett. 501 (2011) 358.
[13] B. Guchhait, S. Daschakraborty, R. Biswas, J. Phys. Chem. B, unpublished data.
[14] M.D. Ediger, Annu. Rev. Phys. Chem. 51 (2000) 99.
[15] W. Huang, R. Richert, Phil. Mag. 87 (2007) 371.
[16] D. Chakrabarti, B. Bagchi, Phys. Rev. Lett. 96 (2006) 187801.
[17] Y. Wang, G.A. Voth, J. Am. Chem. Soc. 127 (2005) 12192.
[18] J.A.C. Lopes, A.A.H. Padua, J. Phys. Chem. B 110 (2006) 3330.
[19] A. Triolo, O. Russina, B. Fazio, R. Triolo, E.D. Cola, Chem. Phys. Lett. 467 (2008) 362.
[20] P.K. Mandal, M. Sarkar, A. Samanta, J. Phys. Chem. A 108 (2004) 9048.
[21] H. Jin, X. Li, M. Maroncelli, J. Phys. Chem. B 111 (2007) 13473.
[22] D.K. Sasmal, A.K. Mandal, T. Mondal, K. Bhattachrayya, J. Phys. Chem. B 115 (2011) 7781.
[23] A. Rahman, Phys. Rev. 136 (1964) 405.
[24] J.P. Hansen, I.R. McDonald, Theory of Simple Liquids, second ed., Academic Press, London, 1986.
[25] J. Habasaki, K.L. Ngai, J. Non-Cryst. Solids 352 (2006) 5170.
[26] F. Faupel, W. Frank, M.-P. Macht, H. Mehrer, V. Naundorf, K. Ratzke, H.R. Schober, et al., Rev. Mod. Phys. 75 (2003) 237.
[27] D. Roy, N. Patel, S. Conte, M. Maroncelli, J. Phys. Chem. B 114 (2010) 8410.
[28] M.G. Del Popolo, G.A. Voth, J. Phys. Chem. B 108 (2004) 1744.
[29] J. Habasaki, K.L. Ngai, Phys. Chem. Chem. Phys. 9 (2007) 4673.
[30] J. Habasaki, K.L. Ngai, Y. Hiwatari, J. Chem. Phys. 121 (2004) 925.
[31] C. Cramer, S. Bruckner, Y. Gao, K. Funke, Phys. Chem. Chem. Phys. 4 (2002) 3214.
[32] K. Ueno, C.A. Angell, J. Phys. Chem. B 115 (2011) xxxx. doi:jp111398r.
[33] A. Muthukumar, J. Phys. A Math. Gen. 14 (1981) 2129.
[34] J. Habasaki, Y. Hiwatari, Phys. Rev. E 62 (2000) 8790.
[35] M.P. Allen, D.J. Tildesley, Computer Simulations of Liquids, Oxford University Press, New York, 1987.
[36] A. Aguado, P.A. Madden, J. Chem. Phys. 119 (2003) 7471.
[37] B. Peterson, J. Saykall, M. Mucha, P. Jungwirth, J. Phys. Chem. B 109 (2005) 10915.
[38] P. Kumar, M. Maroncelli, J. Chem. Phys. 103 (1995) 3038.
[39] P. Jedlovszky, A. Idrissi, J. Chem. Phys. 129 (2008) 164501.
[40] R. Biswas, B. Bagchi, Acc. Chem. Res. 31 (1998) 181.
[41] A.S. Clarke, H. Jonsson, Phys. Rev. E 47 (1993) 3975.
[42] E. Sim, A.Z. Patashinski, M.A. Ratner, J. Chem. Phys. 109 (1998) 7901.
[43] S. Mahiuddin, Can. J. Chem. 74 (1996) 760.
[44] R.A. Wallace, J. Phys. Chem. 75 (1971) 2687.
[45] W.D. Williams, J.A. Ellard, L.R. Dawson, J. Phys. Chem. 79 (1957) 4652.
[46] W. Kob, C. Donati, S.J. Plimpton, P.H. Poole, S.C. Glotzer, Phys. Rev. Lett. 79 (1997) 2827.
[47] J. Habasaki, K.L. Ngai, J. Chem. Phys. 129 (2008) 194501.
[48] S. Bhattacharyya, B. Bagchi, Phys. Rev. Lett. 89 (2002) 025504.
[49] S.M. Bhattacharyya, B. Bagchi, P.G. Wolynes, Proc. Natl. Acad. Sci. USA 105 (2008) 16077.
[50] S.M. Bhattacharyya, B. Bagchi, P.G. Wolynes, J. Chem. Phys. 132 (2010) 104503.